ISSN 2063-5346

EFFECT OF NiO SUBSTITUTION ON THE DIELECTRIC AND MAGNETIC PROPERTIES OF $ZnFe_2O_4$ PREPARED BY WET-CHEMICAL METHOD

Syeda Ayesha

Department of Chemistry, Govt. First Grade College, Kuvempunagar, Mysore-570023, Karnataka, India.

Raviraja S

Department of Physics, Govt. First Grade College, Uppinangady-574241, Dakshina Kannada, India.

Shilpa S

Department of Physics, Govt. First Grade College, Kadugudi, Bengaluru-560067, Karnataka, India.

S. Abdul Khader

Department of Physics, Maharani's Science College for Women (Autonomous), J. L. B Road, Mysore-05.

Asiya Parveez

Department of Physics, Govt. Science College, Chitradurga-577501, Karnataka, India.

Rajeev Ranjan Sinha*

Department of Physics, S. K. M University, Dumka-814101, Jharkhand, India.

Corresponding Author Email: rrsphy@gmail.com

Article History: Received: 04.02.2023 **Revised:** 25.04.2023 **Accepted:** 22.05.2023

ABSTRACT

This article presents the effect of NiO, a transitional metal oxide substitution on dielectric and magnetic studies of zinc ferrite ($ZnFe_2O_4$). NiO was substituted in pure zinc ferrite ($ZnFe_2O_4$) samples with the basic composition (1-x) $ZnFe_2O_4$ + (x) NiO (here, x= 0.0, 0.05, 0.1, and 0.15), were synthesized by wet chemical method using auto-combustion method with the help of the precursors such as nitrates and an organic fuel such as citrate in this case. As-prepared samples were sintered at 900^0C and investigated for various properties. Confirmation of the phase of

the synthesized samples was done by X-ray diffraction (XRD) studies. Peaks observed in the XRD spectrum confirms the single phase spinel cubic structure for the NiO substituted $ZnFe_2O_4$. Using scanning electron microscopy, surface morphology of the samples has been investigated. Frequency dependent dielectric response of the samples were studied using HIOKI make LCR meter model 3520-50 from 100Hz to 5 MHz. Dielectric response has been explained on the basis of Maxwell-Wagner polarization. Magnetic properties of the NiO substituted $ZnFe_2O_4$ samples at RT were measured using vibrating sample magnetometer.

KEYWORDS: Composition; Spinel; Organic; LCR; Magnetic.

1. INTRODUCTION

Mostly used ferrites in the ferrite family are spinel ferrites. Nano structured soft spinel ferrites have attracted great interest due to their excellent physio-chemical properties such as , low toxicity and their magnetism as well as, because of their highly tunable properties, like its dielectric, magnetic properties, which can be easily modified just adopting various preparation techniques and various factors such as the type of organic fuel used for the synthesis, P_H of the redox solution, composition of the metal ions, crystal structure, types of additives and sintering temperature etc [1-3]. Nano-structured magnetic oxides are currently considered among the widely successful magnetic nanoparticles (MNPs) that can be extensively used for various technological and in medical applications such as electrochemical sensor applications, in storage medium, contrast enhancement in magnetic resonance imaging, suspension systems using magnetic fluids, targeted drug delivery and in many more technological devices and applications. [4-5].

Spinel magnetic oxide materials, mainly consists of Fe_2O_3 and have spinel (MFe_2O_4) cubic structure, here M represents to a divalent metal ion(s). These samples, which are ferri-magnetic in nature exhibit magnetic hysteresis (M-H curve) and at the same time exhibit spontaneous magnetization. Various properties of magnetic spinel is because of distribution of metal ions among the available voids such as tetrahedral (A) and octahedral (B) sites [6]. For any materials of interest, its properties are highly dependent on preparation technique selected, type of synthesis environment such as in inert or in open air atmosphere, type of organic fuel used, sintering time and temperature, etc.

In $ZnFe_2O_4$, oxygen atoms form face-centered cubic (FCC) packing, while **Fe** and **Zn** occupy octahedral and tetrahedral sites. A unit cell of a spinel structure consists of a total 64 sites contributed from eight FCC cells, out of which 56 sites occupied and the remaining 8 cells are vacant. Depending on how Zn ions occupy different sites, a spinel structure can be either a normal or inverse [7-9]. One-unit cell consists of eight molecules of of $ZnFe_2O_4$ or 56 ions out of which eight are Zn^{+2}, 32 are O^{-2} and 16 are Fe^{+3}. All tetrahedral (A- sites) are occupied by Zn^{+2} ions and all octahedral (B-sites) are occupied by Fe^{+3} in the normal spinel structure of $ZnFe_2O_4$.

Cation distribution in the respective sites are responsible for the magnetic and electrical properties displayed by ferrites. When dopants are added to control the size or morphology of the nanoparticles, the distribution of cations is disturbed. Any alteration caused by dopants in any or both the sites tends to modify their magnetic and electrical properties finally resulting in modified material behavior [10-11].

Among metal oxides of technological importance, NiO is a transitional metal oxide which is anti-ferromagnetic in nature below 523 kelvin and is an excellent material for catalysis, energy conversion, in

storage devices, gas sensors and electro-chromic films etc [11].

In our present study, samples of NiO transitional metal oxide substituted zinc ferrite with the basic composition (1-x) $ZnFe_2O_4$ + (x) NiO (here, x= 0.0, 0.05, 0.1, and 0.15), were prepared by wet-chemical method using nitrate-citrate auto-combustion method. This method is a self-propagating thermally-induced reaction of a gel, obtained from aqueous solutions containing metallic nitrates which acts as oxidizer and an organic fuel. Stoichiometric proportions between fuel and metallic nitrates are calculated according to the valencies of the reacting elements so as to provide the relation of oxidizer/fuel equal to one [12]. Here, metallic nitrates are preferred as starting materials which are also known as precursors, because of their water-soluble nature, have low ignition temperatures and are easy to prepare.

2. MATERIALS AND METHODS

Nano-powders of transitional metal oxide (NiO) substituted $ZnFe_2O_4$ ferrite samples of basic chemical composition (1-x) $ZnFe_2O_4$ + (x) NiO (here, x= 0.0, 0.05, 0.1, and 0.15) were prepared using auto-combustion method. Precursors for starting the materials synthesis using the combustion method are Ferric Nitrate ($Fe(NO_3)_2.9H_2O$), Zinc Nitrate ($Zn(NO_3)_2.6H_2O$) Nickel Nitrate ($Ni(NO_3)_2.6H_2O$) and Citric acid ($C_6H_8O_7.H_2O$), all chemicals are of AR Grade with purity more than 99%. Aqueous solutions of metallic nitrates and Citric acid, which is here taken as organic fuel needed for auto-combustion reaction and are taken as per the stoichiometry. Equi-molar citric acid was added into the aqueous solution of metallic nitrates. Aqueous solution containing redox mixture was taken in a silica crucible and is allowed in to a muffle furnace, which was already pre-heated to a temperature of 500^0C. Redox mixture finally yields porous and fluffy voluminous ferrite powder. Obtained fluffy material was ground to get ferrite powders. As-burnt ash was sintered at 900^0C for 4 hours to get better crystallization and homogeneous cation distribution in the proposed spinel and finally ground to get proposed ferrite nano-powders.

Phase confirmation of the proposed samples were investigated using X-ray diffraction (XRD) studies using Bruker AXS D8 Advance X-ray diffractometer (using Cu-K_α radiation, λ=1.5406 Å), a working voltage of 40kV at 40mA of current. Diffraction data were collected in the 2θ range 10-70^0. Morphology of the sintered samples has been investigated using Field Emission Scanning Electron Microscope (JEOL Model 7610FPLUS). Magnetic measurements were performed using vibrating sample magnetometer VSM, Lakeshore Model: 7400, USA. Parallel capacitance, C_p and dissipation factor, tanδ as a function of frequency in the range 100 Hz-5 MHz were measured using a precision LCR meter. Real and imaginary parts of dielectric permitivity (ε' and ε'') dielectric permitivity (ε') and (ε'') were computed using the formulae [13],

$$\varepsilon' = Ct/\varepsilon_0 A \quad (1)$$

$$\varepsilon'' = \varepsilon' \tan\delta \quad (2)$$

Where, t is the thickness and A, the area of the pellet.

The ac conductivity, σ_{ac} was determined from the dielectric loss factor using a relation

$$\sigma_{ac} = \omega \varepsilon_0 \varepsilon'' \quad (3)$$

Where, ε_0 is the vacuum permittivity and $\omega = 2\pi f$ with f being frequency.

3. RESULTS AND DISCUSSION

3.1 PHASE AND SURFACE MORPHOLOGY

XRD Patterns of the proposed samples of the NiO metal oxide substituted $ZnFe_2O_4$ system with basic chemical composition (1-

x) $ZnFe_2O_4$ + (x) NiO (here, x= 0.0, 0.05, 0.1, and 0.15) are presented in Figure 1. Presence of (220), (311), (400), (422), (511), (440) and (533) planes indexed for the cubic phase of spinel ferrites. Whereas presence of (111), (220) and (222) planes are indexed for NiO. All proposed nano-ferrite samples exhibited Fd-3m space group, which is confirmed by the JCPDS Card No: 22-1012 for the $ZnFe_2O_4$. Peaks of NiO have single phase face centered cubic structure, which is confirmed by the JCPDS Card No:71-1179. As the NiO concentration in $ZnFe_2O_4$ increases, its corresponding peak intensity also slightly increases. Here in XRD spectrum, NiO is represented by an asterisk (*) symbol. Synthesized samples are labelled as ZFNiO1, ZFNiO2 and ZFNiO3 for 5 % wt NiO, 10% wt NiO and 15 % wt NiO in the pure $ZnFe_2O_4$. Optical micrographs of the sintered samples are depicted in Fig. 2 (a-c), shows the surface structure for the proposed samples. All the samples are having well dispersed and agglomeration structures.

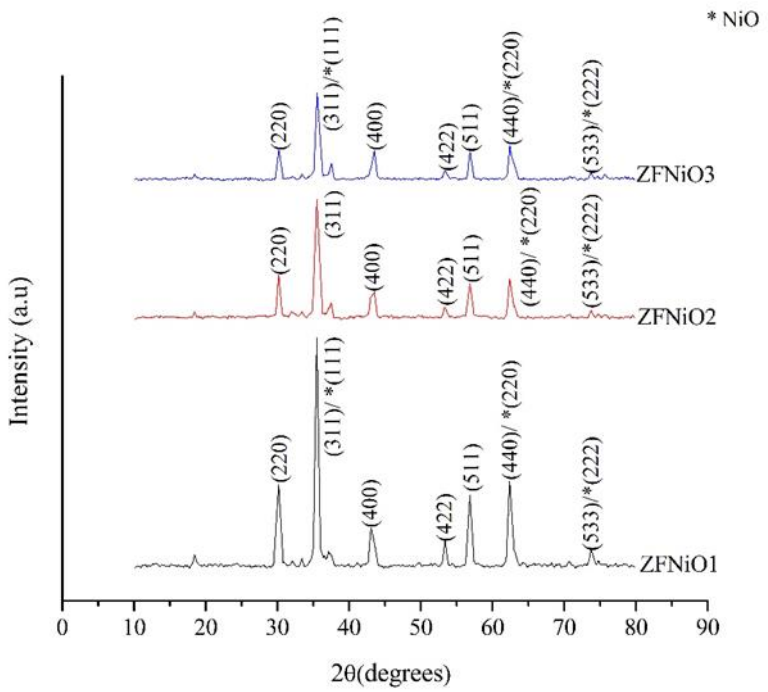

Fig. 1. XRD Patterns of transitional metal oxide-NiO substituted $ZnFe_2O_4$

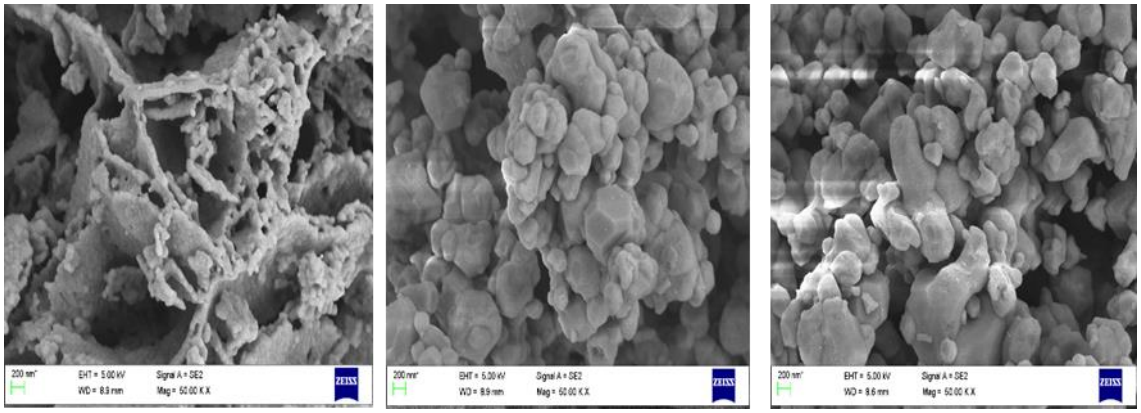

Fig. 2 Micrographs of NiO substituted in $ZnFe_2O_4$ (a) 5% wt in ZFO (b) 10% wt in ZFO (c) 15% wt in ZFO

3.2 DIELECTRIC AND IMPEDANCE STUDIES

Dielectric response of the proposed samples in the frequency range from 100 Hz to 5 MHz were probed using HIOKI LCR meter to know the inductive, capacitive and resistive nature of the samples. Various dielectric parameters such as permittivity, ε' and ac conductivity (σ_{ac}) with respect to variation in frequency at room temperature for the synthesized samples is shown in Fig.3. From the Fig.3 (a), it is clear that ε' decreases with increasing frequencies and remains almost independent at higher frequencies. Variation of dielectric constant with applied frequency is due to charge transport relaxation. Dielectric dispersion is common in ceramics like ferrites and is attributed to Maxwell and Wagner type of interfacial polarization [14-15], as the dielectric constant is a combined effect of dipolar, electronic, ionic and interfacial polarizations. Since ionic polarization decreases with frequency, at higher frequency cycle rates, the constituent electric dipoles are unable to follow the quick variations of the alternating applied electric field and hence, measured ε' also decreased with frequency. Larger values of permittivity are related with space charge polarization at grain boundary and heterogeneous dielectric structure [16-17].

Variation in the dielectric loss for all the proposed series of samples upto the frequency range of 5 MHz at room temperature is shown in Fig. 3(b). Values of loss tangent (tanδ) represent the attenuation in these proposed ceramics and polarization being unable to respond to applied external frequency. Similar nature of curves for both ε' and tanδ are almost similar and may be correlated to the domain wall motion with the applied field, the electron exchange between Fe^{+2} and Fe^{+3} ions can correlate with the dielectric properties exhibited by proposed samples.

In order to understand the type of charge carriers and type of polarons responsible for conduction, ac conductivity, σ_{ac} were estimated as per $\sigma_{ac}= \omega \varepsilon_0 \varepsilon''$, with ε_0 is the permittivity of free space and $\omega=2\pi f$.

For the synthesized samples, variation of a.c conductivity, σ_{ac} with frequency, ln (ω), is shown in Fig.3 (c). Obtained plots are almost linear for the entire range of frequency except at lower frequencies. Linear variation of σ_{ac} with frequency confirms that, conduction in mixed spinel ferrite occurs by the hopping of charge carriers between the localized states which confirms the small polaron type of conduction [18]. Conduction mechanism in spinel ferrites can be explained based on the hopping of charge carriers between Fe^{+2} and Fe^{+3} ions on octahedral lattice sites. Increase in the frequency of the applied field accelerates the hopping of charge carriers thereby enhancing the overall conduction process, thereby increasing the conductivity. At higher frequencies, ac conductivity (σ_{ac}), remains constant because the hopping frequency of the charge carriers no longer follows the external applied field variations and lags behind it. However, the decrease in conductivity values at lower frequencies can be correlated to conduction by mixed polarons.

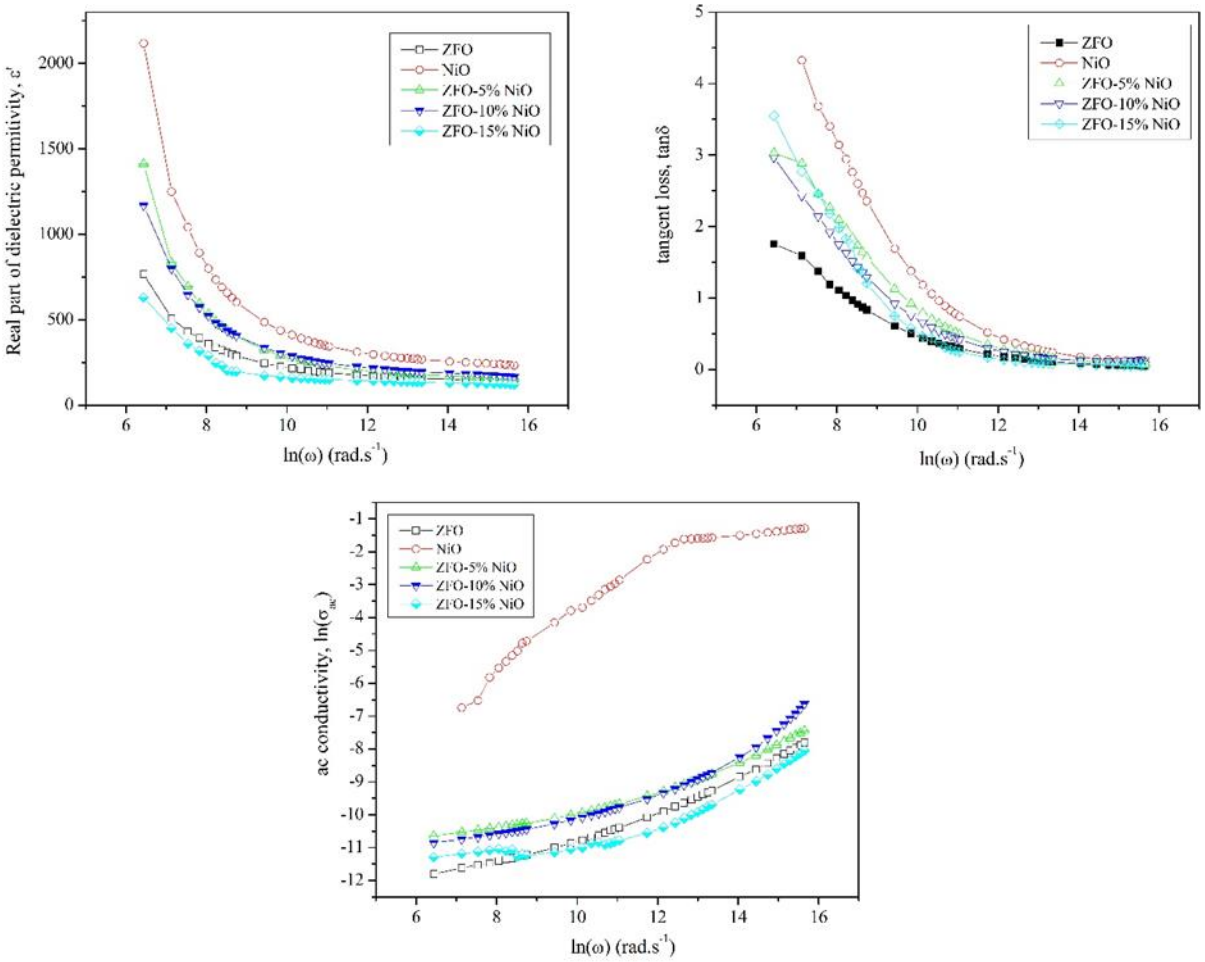

Fig. 3 Variation of (a). Real Part of Dielectric permitivity, **ε'** with **ln(ω)** and (b) Tangent loss factor **tanδ** with **ln(ω)** and (c) AC conductivity, **ln (σ_{ac})** with **ln(ω).**

3.3 MAGNETIC STUDIES OF ZFO-NiO SYSTEM

M-H loops, at RT were recorded for all the three transitional metal oxide- NiO substituted samples and are shown in Fig.4. From, M-H loops, it is clear that loops are saturated at higher field values, which is the characteristic feature of any ferromagnetic material. Proposed samples exhibited no hysteresis, which may be attributed to super paramagnetic nature of the samples. Magnetic parameters such as M_S, M_r and H_c were extracted from the obtained M-H loops [19-20]. Here M_S, H_c, M represents saturation magnetization, applied magnetic field and magnetization. Measured magnetic parameters for all the samples under the applied magnetic field (H) are summarized in Table 1. Proposed samples are found to be having very low values of Mr and Hc, which is an essential characteristic of any magnetic material, so that it can be used in a wide range of electronic and smart appliances.

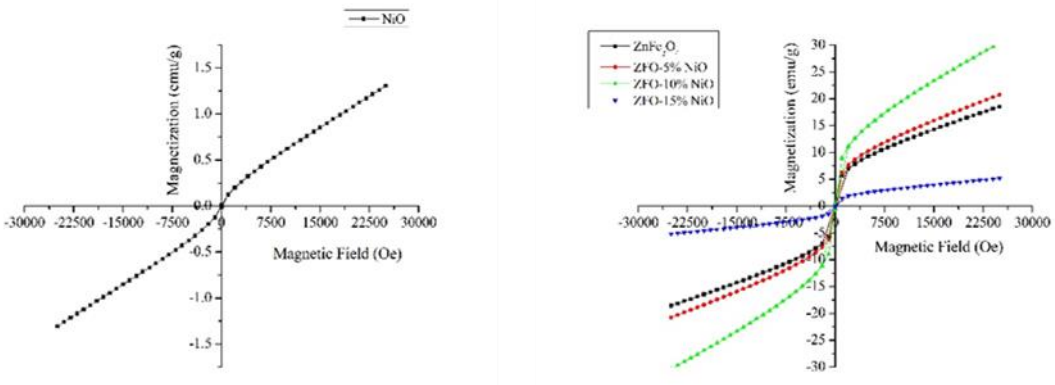

Fig. 4. Magnetic Hysteresis loops of NiO substituted $ZnFe_2O_4$ Nano-powders.

Table 1. Magnetic parameters obtained from M-H Loops.

Sample(s)	Saturation Magnetization **M_s** (emu/g)	Remanent Magnetization **M_r** (emu/g)	Coercive Field **H_c** (Oe)
$ZnFe_2O_4$	18.55	0.24	98.87
NiO	1.34	0.013	85
5% wt NiO – $ZnFe_2O_4$	20.75	0.21	10
10 % wt NiO- $ZnFe_2O_4$	29.70	0.27	1.5
15 % wt NiO- $ZnFe_2O_4$	5.16	0.06	56.36

CONCLUSIONS

Effect of the NiO substitution in ferrite phase ($ZnFe_2O_4$) of the basic chemical composition system, with the general formula, (1-x) $ZnFe_2O_4$ + (x) NiO (here, x= 0.0, 0.05, 0.1, and 0.15) were prepared successfully using auto-combustion method which involves nitrate-citrate precursors. Structural phase is confirmed through XRD studies for the transitional metal oxide NiO substituted $ZnFe_2O_4$ nano samples. Morphology of the nano-powders reveals the dense structures with agglomeration. From magnetic studies, it is observed that, the proposed samples with narrow hysteresis loop were synthesized with low values of coercivity. Hence, these samples are magnetically soft materials. Finally, it is concluded that, TMO(NiO) substituted $ZnFe_2O_4$ nano-powders have been studied for dielectric and magnetic properties.

ACKNOWLEDGEMENTS

Authors are highly thankful to CENSE, IISc-Bangalore for providing PXRD and FESEM facilities to accomplish this research work.

REFERENCES

1. J. L Liu, L. Z Fan and X.Qu Electrochimica, 66, pp.302 (2012).

2. M.Madhukara Naik, H. S Bhojya Naik, G. Nagaraju, M.Vinuth, H.Raja Naika, K.Vinu, Microchem J,146, 1227 (2019).

3. C N Chinnasamy, A Narayanasamy, N. Ponpandian, K.M Chattopadhyay, J.M Greneche, Scr.Mater ,44, 1407 (2001).

4. S R Patade, D. D Andhare, S B Somvanshi, S A Jadhav, M. V Khedkar and K M Jadhav, Ceramic.Int, 46, 25576 (2020).

5. N M Mahmoodi, Mater.Res. Bull, 48, 4255 (2013).

6. M.Bohra, V.Alman, R.Arras, Nanomaterials, 11,1286 (2021).

7. S.Darbagh A, A.Ati, S.K Ghoshal, S Zare, R M Rosnan, Z.Othaman, Bull.Mater.Sci,39, pp.1029-1037 (2016).

8. D D Andhare, Supriya R.P, J S Kounsalye, K M Jadhav, Physica B: Condensed Matter, 583,412051 (2020).

9. A.Kmita, A.Pribulova, M.Holtzer, A.Roczniak, Arch. Metall.Mater ,61, 2141 (2016).

10. S.Abdul Khader, Asiya Parveez, Arka Chaudhuri, M S Shekhawat and T.Sankarappa, Physica B: Condensed Matter, 584, May Issue, pp.411675 (2020).

11. J P Singh, R C Srivastava, H.M Agarwal, P.Chand, Int.J.Nanoscience, 08,523 (2008).

12. Wagner KW (1913) Ann Phys 40:817.

13. Maxwell JC, Electricity & Magnetism, Vol 1, Oxford University Press, Oxford (1929).

14. Koops C G (1951) Phys Rev 83:121.

15. M. Atif, S. K Hasanain, M. Nadeem, Solid State Communications, 138, 416 (2006).

16. J P Singh, R C Srivastava, H.M Agarwal, R P S Kushwaha, P. Chand, R. Kumar , Int.Jour.Nanoscience,07, 21 (2008).

17. Shivkumar Naik, Asiya Parveez, Arka Chaudhuri, S. Abdul Khader, 14, 11(3), pp.12103-12108 (2017).

18. Keerthana S, Yuvakkumar, Ravi G, Pavithra S, Thambidurai M, Dang C, Velauthapillai D, Environ.Res ,200, pp.111528 (2021).

19. Swati Kumari, Vikash Kumar, Pawan Kumar, Manoranjan Kar, Lawrence Kumar, Advanced Powder Technology, 26(1), pp.213-223 (2015).

20. Ali N, Zaman H, Bilal M, Nazir M S, Iqbal H M, Sci.Total Environ, 670, pp.523 (2019).